Metal Ion Interactions with Polyalanine Peptides

Motoya Kohtani and Martin F. Jarrold*,†

Chemistry Department, Indiana University, 800 East Kirkwood Avenue, Bloomington, Indiana 47405-7102

Sheena Wee and Richard A. J. O'Hair*,‡

School of Chemistry, The University of Melbourne, Parkville, Victoria 3052, Australia

Received: January 20, 2004; In Final Form: February 27, 2004

Electrospray mass spectrometry and ion mobility measurements have been used to perform a systematic study of complex formation between metal ions and polyalanine peptides. Monovalent metal ions (Li^+, Na^+, K^+, Cs^+, and Rb^+) are known to form complexes with polyalanine peptides. In the unsolvated complex, the polyalanine peptide adopts a helical conformation that is stabilized by coordination of the metal ion to the C-terminus. Complexes are also observed between polyalanine peptides and the dications of alkali earth metals (Mg^{2+}, Ca^{2+}, Sr^{2+}, and Ba^{2+}), though they are substantially less abundant than with the monovalent ions. Ion mobility measurements for the unsolvated Ala_n+M^{2+} complexes are consistent with an α-helical conformation, but with a substantial disruption of the helix at the C-terminus due to much stronger coordination to the dication. Attempts to observe complex formation with trivalent metal ions (In^{3+}, Sc^{3+}, and Y^{3+}) were not successful.

Introduction

The interaction of polypeptides and proteins with metal ions has been a subject of considerable interest since Hofmeister's pioneering study of the precipitation of hen lysozyme using different salts.[1] The earlier studies focused largely on the effect of ionic strength on the pH dependent denaturation curves of proteins,[2,3,4] and on theoretical models of the metal ion−protein interactions.[5] In recent years, interest in the interaction of metal ions with polypeptides has increased, especially with the advent of de novo protein engineering. Here the side chains usually act as ligands, and the metal ion interactions with the side chains are designed to constrain the geometry. Since the discovery of metal-ion-induced α-helix formation using both natural[6] and unnatural[7] amino acids as ligands, a wide variety of metal interactions with polypeptides and proteins have been designed and explored.[8−14] These studies represent an important step in the conformational engineering of proteins. Alongside these advances, there have been a series of studies of unsolvated peptide−metal ion complexes in the gas phase that have the potential to provide a more detailed understanding of the basic interactions that are present. Metal ion complexes with individual amino acids,[15−18] peptides,[19−25] and proteins[26,27] have been studied. The approaches employed include collision-induced dissociation, blackbody infrared radiative dissociation, and ion mobility measurements. These studies were facilitated by the development of soft-ionization methods, such as electrospray, which make it possible to place large biological molecules and weakly bound complexes into the gas phase where they can be studied in the absence of a solvent. By comparison of the structure of a peptide in the gas phase with its conformation in solution, the structural contribution of the solvent is highlighted.

In a recent communication, we reported that unsolvated Ala_n+M^+ complexes, where M = Li^+, Na^+, K^+, Rb^+, and Cs^+ were α-helical whereas the protonated analogues, Ala_n+H^+, have globular conformations when electrosprayed from solution.[28] The side chain of alanine (a methyl group) is not an effective ligand, and so the interactions between the peptide and the metal ion most likely occur through the backbone carbonyl groups.[29] The helix is stabilized in the Ala_n+M^+ complexes because the metal ion binds to the dangling carbonyl groups at the C-terminus, where the charge interacts favorably with the helix macrodipole. Alanine is known to have a high helix propensity.

In the present work we extend these studies to examine the interactions of metallic dications and trications with polyalanine peptides. The metals studied here include several that have important roles in biological systems. One might expect that the additional charge would favor more extensive solvation by peptide carbonyl groups, leading to a globular conformation with a central metal ion surrounded by the peptide. However, this is not the case. For the dications, Ala_n+M^{2+} where M = Mg^{2+}, Ca^{2+}, Sr^{2+}, and Ba^{2+}, experimental results and simulations show that the peptide adopts an α-helical conformation, albeit significantly deformed at the metal binding site. For the trications, M^{3+} = In^{3+}, Sc^{3+}, and Y^{3+} no discernible metal−peptide complex was ever obtained with the polyalanine peptides.

Experimental Methods

All measurements were performed on a custom built ion mobility mass spectrometer consisting of an electrospray source and a temperature variable drift tube, followed by quadrupole mass spectrometer and ion detector. The apparatus has been described in detail elsewhere.[30] Briefly, the peptides are electrosprayed in air and enter the apparatus through a heated capillary interface. After passing through a short differentially pumped region, the ions are focused into the drift tube, which contains helium buffer gas at around 4.0 Torr. A weak electric field gently pulls the ions through the buffer gas at a velocity

† E-mail: mfj@indiana.edu.
‡ E-mail: rohair@unimelb.edu.au.

10.1021/jp049708g CCC: $27.50
Published on Web 04/22/2004

that is inversely proportional to their average collision cross section. The collision cross section is similar to the average two-dimensional area "swept-out" by the ion as it travels through the buffer gas, except that intermolecular forces between the peptide ion and helium gas must also be taken into account. Compact ions travel across the drift tube more rapidly than elongated conformations such as helices, and so it is possible to separate out different conformations of the same peptide. After traveling across the drift tube, some of the ions exit through a small aperture and are focused into a quadrupole mass spectrometer. The mass analyzed ions are then detected with a collision dynode and a pair of microchannel plates. The drift times, the amount of time it takes for ions to travel across the drift tube, are determined by injecting a short pulse of ions and recording their arrival time distribution at the detector. The drift times can be converted to average collision cross sections using well-established expressions.[31] To assign the features observed in the experiments, the measured collision cross sections are compared to average cross sections calculated for conformations derived from molecular dynamics simulations. The ion mobility experiments are conducted under low-field conditions where frictional heating and alignment of the ions in the electric field are negligible.

All peptides were synthesized using *FastMoc* chemistry on an Applied Biosystems model 433A peptide synthesizer. After cleavage with a mixture of 95% trifluoroacetic acid and 5% water, the peptides were precipitated, centrifuged, and lyophilized. Electrospray solutions were prepared by dissolving 1 mg of peptide in 1 mL of TFA and 0.1 mL of purified water (TFA was used as a solvent because the peptides are at best marginally soluble in water and methanol). The appropriate chloride salt was then added to bring the metal ion concentration to the optimum range of around 10^{-3} M. All of the salts employed here were obtained from Sigma-Aldrich.

Experimental Results

Ala_n+M^{2+} complexes were observed with M = Mg^{2+}, Ca^{2+}, Sr^{2+}, and Ba^{2+}. Only a single narrow feature was observed in the drift time distributions for all of them. Figure 1 shows the relative collision cross sections determined from the drift times for the Ala_n+M^{2+} complexes plotted against the number of alanine residues, n, for $n = 14-25$. The relative cross sections (in Å^2) are obtained from CS(Relative) = CS(Exp) − 14.5n, where CS(Exp) is the measured collision cross section (in Å^2) and 14.5 is the average cross section increment per residue determined (from calculations) for an ideal polyalanine α-helix. Peptides with α-helical conformations have relative cross sections that are constant as the number of residues varies, whereas for peptides with more compact globular conformations (closely packed, random-looking three-dimensional structures) the relative cross sections decrease as the peptide size increases. Thus using this relative cross section scale it is easy to distinguish between helical and globular conformations, which are the two main types of structures observed for the peptides in the size range examined here. Previously reported results for Ala_n+H^+ and Ala_n+Na^+ are shown in Figure 1 to illustrate both cases: the relative cross section for the Ala_n+H^+ peptides decreases sharply with increasing peptide length, which is characteristic of globular conformations, whereas for Ala_n+Na^+ the relative cross sections are almost independent of the number of residues, which is characteristic of an α-helix. Results for the other monovalent metals studied (Li^+, K^+, Cs^+, and Rb^+) are virtually identical to those for Ala_n+Na^+ (except for the small lithium complexes). The results for the polyalanine peptides coordinated to the alkali earth dications, Ala_n+M^{2+}, resemble those for the Ala_n+Na^+ complexes: the relative cross sections are almost independent of peptide length; which suggests that the Ala_n+M^{2+} species are helical. However, the relative cross sections for the Ala_n+M^{2+} peptides are consistently smaller than the corresponding values for the Ala_n+Na^+ peptides by about 10 Å^2. This suggests a systematic difference in their conformations.

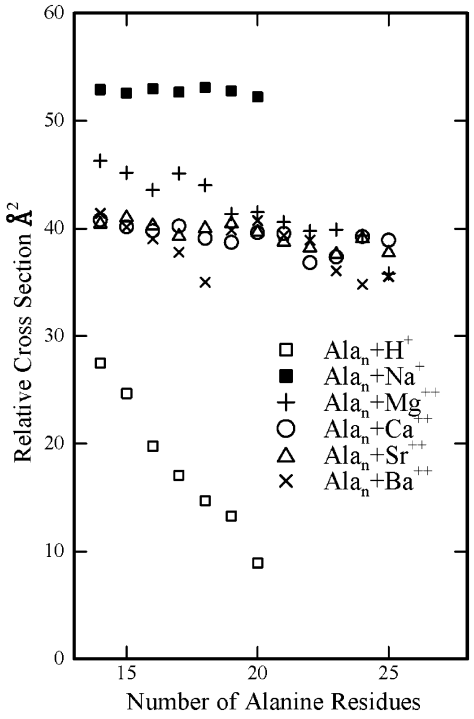

Figure 1. Plot of the relative collision cross section (in Å^2) against the number of alanine residues for Ala_n+H^+, Ala_n+Na^+, and Ala_n+M^{2+} where $M^{2+} = Mg^{2+}$, Ca^{2+}, Sr^{2+}, and Ba^{2+}. The relative cross sections were calculated from CS(Relative) = CS(Experimental) − 14.5n, where n is the number of alanine residues, and 14.5 Å^2 is the increment in the average cross section per alanine residue determined (from calculations) for an ideal α-helix.

The relative abundances for the metal ion complexes were obtained by comparing the measured intensity of the metal−peptide complex to the intensity of the protonated peptides, Ala_n+H^+, in the mass spectrum. For solutions prepared under identical conditions with the same metal ion concentration the relative abundances of the complexes of the divalent metals (Mg^{2+}, Ca^{2+}, Sr^{2+}, and Ba^{2+}) are substantially (around a factor of 5) lower than with the monovalent metals (Li^+, Na^+, K^+, Cs^+, and Rb^+). Singly charged (peptide$-H^+$)$+M^{2+}$ complexes were not observed. Complexes of the trivalent metal ions (In^{3+}, Sc^{3+}, and Y^{3+}) were not observed under any conditions despite a thorough search with a wide range of salt concentrations.

Molecular Dynamics Simulations

Molecular dynamics (MD) simulations were performed for $Ala_{20}+Ca^{2+}$. The simulations were done using the MACSIMUS suite of programs[32] with the CHARMM force field (21.3 parameter set). Simulated annealing runs were performed with a cooling schedule consisting of a gradual descent from 600 to 300 K over 915 ps with brief +200 K temperature spikes, which enable the system to climb out of undesirable local minima.[33] Forty simulations were performed starting from a fully extended (φ, ψ = 180°) starting structure. These runs differed only in the initial placement of the calcium dication. Twenty simulations were performed with the calcium dication near the C-terminus

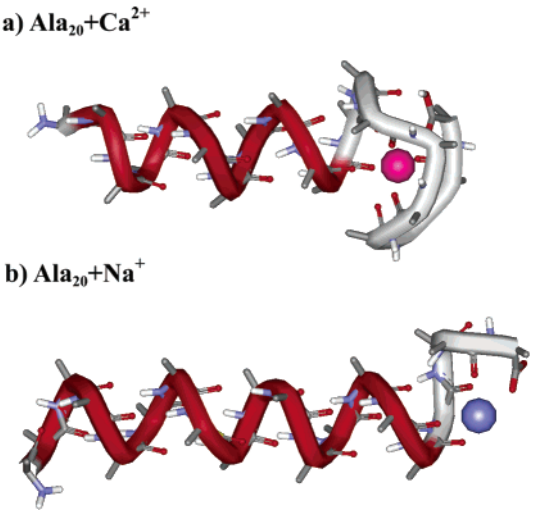

Figure 2. Lowest energy conformations found in the molecular dynamics simulations of (a) $Ala_{20}+Ca^{2+}$ and (b) $Ala_{20}+Na^{+}$. In both cases the calculated cross sections matched the measured ones to within 2%. The structure for $Ala_{20}+Na^{+}$ was taken from ref 28.

carbonyl. Ten runs each were performed with the ion placed near the middle (carbonyl of the tenth alanine) and near the N-terminus (carbonyl of the first alanine residue). Ten additional runs were performed with an α-helical starting structure with the calcium dication near the C-terminus. The average energy of the final conformation was determined from the last 35 ps of the simulation. Average collision cross sections were calculated from 50 snapshots taken from the last 35 ps. The cross sections were calculated using the empirically corrected exact hard sphere model.[34] If the conformation is correct, the calculated cross section is expected to be within 2% of the experimental value. To perform the cross section calculations, it was necessary to determine a value for the Ca^{2+}-He hard sphere collision distance. An estimate was obtained from the interaction potential calculated using Jaguar v. 4.1 (Schrodinger, Inc.) with a B3LYP/LACVP**++ effective core potential[35] for Ca^{2+} and 6-31G**++ for He. Because there is only one Ca^{2+} coordinated to the peptide and it is buried in most of the conformations, the calculated cross section is not sensitive to the Ca^{2+}−He hard sphere collision distance.

Two main groups of structures were found in the simulations: helices and globules. The helices are around 70 kJ mol^{-1} lower in energy than the nonhelical structures. Because of its relatively high charge, the calcium ion is not very mobile in the simulations and only those simulations that started with the calcium ion near the C-terminus produced helices. The other simulations where the calcium ion was initially placed in the center of the peptide and at the N-terminus produced globular conformations with minimal helicity. This observation is consistent with the view that the charge must be located at the C-terminus to stabilize the helix.

The lowest energy conformation found in the MD simulations for $Ala_{20}+Ca^{2+}$ is shown in Figure 2. The structure is α-helical with the exception of the C-terminal region where coordination of the calcium ion causes considerable disruption of the regular α-helical structure. All the low energy helical conformations found in the MD simulations for $Ala_{20}+Ca^{2+}$ have a similar structure. The calculated collision cross section for the structure shown in Figure 2 is 328.9 $Å^2$, a value in excellent agreement with the experimental value of 329.6 $Å^2$. Moreover, the calculated cross section is in good agreement with the cross sections for all the other alkali earth metal ion adduct of Ala_{20}, suggesting that they all have structures that are similar to the one shown in Figure 2.

Discussion

In the structure shown in Figure 2a for $Ala_{20}+Ca^{2+}$ the C-terminus end of the helix (from residue 12 to 20) is disrupted and wrapped around the Ca^{2+} ion. Thus there are potentially eight carbonyl groups coordinated to the ion. A coordination number of eight is common for Ca^{2+}. However, the coordination provided by the peptide is not ideal because of the constraints posed by the backbone, and several of the eight carbonyl groups are not pointing directly at the metal. A better coordination of the metal ion might be achieved by disrupting more of the α-helical region of the peptide. However, the final conformation of the complex is probably determined by a balance between maximizing the metal coordination and minimizing the disruption to the α-helical regions. The helix macrodipole is expected to scale with the length of the helix (for short helices) so making the helix longer increases the interaction between the helix macrodipole and the charge on the metal ion.

In calcium binding proteins, the calcium is usually seven-coordinate, though six-coordinate calcium also occurs.[36] Intracellular proteins that reversibly bind Ca^{2+} have a common binding motif of two helices flanking a 12-residue loop from which the oxygen ligands that bind the calcium ion are derived. This motif is often referred to as an "EF-hand" with an index finger (the E-helix), a curled second finger (the loop), and a thumb (the F-helix). It has been reported that binding La^{3+} (which is known to be an excellent substitute for calcium) to a synthetic peptide consisting of a 12-residue calcium binding loop with a A_4Q block attached to the C-terminus induces an α-helix in the last seven residues (the underlined portion of Ac-**DKDGDGYIS<u>AAE</u>**<u>AAAQ</u>-NH_2, the bold portion is the calcium binding loop). In this peptide the metal is bound at the N-terminus end of the helix, whereas in the $Ala_{20}+Ca^{2+}$ complex the simulations suggest that the metal binds to the C-terminus end of the helix. This arrangement is preferred in the Ala_n+Ca^{2+} complexes because the positive charge is located at the C-terminus of the helix where it can undergo favorable interaction with the helix dipole (the polyalanine peptides do not possess a tailored calcium binding site). Furthermore, coordination of the backbone carbonyl groups to the metal means that the backbone amide groups are pointing away from the metal and are at least partly templated for helix formation.

The structures of the complexes of the other divalent metal ions (Mg^{2+}, Sr^{2+}, and Ba^{2+}) with polyalanine are expected to be similar to that for $Ala_{20}+Ca^{2+}$ because they all have similar cross sections in the experiments. The smaller Ala_n+Mg^{2+} complexes are a possible exception: the small Mg^{2+} ion is known to prefer a coordination number of 6.[37] The slightly elevated relative cross sections observed for the Ala_n+Mg^{2+} complexes with $n < 19$ compared to those for the other divalent metals (see Figure 1) may indicate that these complexes tend toward slightly fewer residues in the coordination shell and less disruption of the helix.

Figure 2b shows the lowest energy conformation found for $Ala_{20}+Na^{+}$ in previous studies of the interactions of the monovalent metal ions (Li^{+}, Na^{+}, K^{+}, Cs^{+}, and Rb^{+}) with polyalanine peptides. In the $Ala_{20}+Na^{+}$ complex, the polyalanine peptide is α-helical up to about residue 17. The structures of the complexes for the other monovalent metal ions (Li^{+}, K^{+}, Cs^{+}, and Rb^{+}) are expected to be similar because they have similar cross sections (except for the smaller Ala_n+Li^{+} complexes that have smaller cross sections and may adopt globular

conformations). The calculated cross section for the $Ala_{20}+Na^+$ complex shown in Figure 2b matches the measured value for this peptide. Thus the difference in the measured cross sections of the monovalent and divalent metal ion complexes reflects the greater degree of disruption of the α-helix by the divalent metal ions. More unraveled conformations similar to that shown in Figure 2a for $Ala_{20}+Ca^{2+}$ were also found in the simulations for the $Ala_{20}+Na^+$ complex. However, they were around 60 kJ mol^{-1} higher in energy than the less unraveled complex shown in Figure 2b. Less unraveled conformations, analogues of the lowest energy $Ala_{20}+Na^+$ helical structure, were not observed in the simulations for $Ala_{20}+Ca^{2+}$, indicating that they must be significantly higher in energy than the more unraveled conformations preferred by the divalent metals. The difference in the preferred conformations of the monovalent and divalent metal ion complexes can be understood in terms of the balance between maximizing the metal coordination and minimizing the disruption to the α-helical regions.

The complexes of the divalent metals (Mg^{2+}, Ca^{2+}, Sr^{2+}, and Ba^{2+}) are significantly less abundant than the complexes of the monovalent metals (Li^+, Na^+, K^+, Cs^+, and Rb^+), and for the trivalent metal ions (In^{3+}, Sc^{3+}, and Y^{3+}) the complexes were not observed. Thus there is a clear trend with the abundances of the complexes, with $M^+ > M^{2+} > M^{3+}$. The interaction between the unsolvated peptide and metal ion must increase as the charge increases; so the absence of the $Ala_{20}+M^{3+}$ complexes is not because they are intrinsically unstable. So either these complexes are not formed in solution or there is some feature of the electrospray process that discriminates against them.

The second and third ionization energies of most metals are greater than the ionization energies of common solvents; thus bare M^{2+} and M^{3+} ions are usually reduced on contact with a solvent molecule.[38] Solvated M^{2+} and M^{3+} ions can be prepared by electrospray. However, the preparation of solvated M^{3+} ions has remained a challenge and charge-reduced species that incorporate an anion such as $[MX(HOR)_n]^{2+}$ or $[MOR(HOR)_n]^{2+}$ are usually observed.[39] In the present case, the failure to observe Ala_n+M^{3+} directly or their charge reduced analogues raises the possibility that complexes between the trivalent metal ions and the peptides are not abundant in solution.

The formation of a complex between a metal ion and a peptide in solution depends primarily on a thermodynamic balance between the hydration energy lost when the ion is desolvated to form the complex, and the energy gained by complexing the metal ion with the peptide. For the trivalent metals the high hydration energies of the metal ion may not be fully recovered by interactions with the peptide. However, the situation must be more favorable for the singly charged metals. Abundant Ala_n+M^+ complexes are observed even with very low salt concentrations; indeed, sodium and potassium complexes are often observed in mass spectra as a result of trace impurities (in other words, without the addition of salt). These observations suggest that the Ala_n+M^+ complexes may be present in solution, rather than just formed during the electrospray process. There is a synergistic stabilization of the helical Ala_n+M^+ complexes where coordination of the oxyphilic metal ions by the dangling CO groups at the C-terminus not only caps the helix but leads to favorable interaction of the charge with the helix macrodipole.

Conclusions

We have performed a systematic study of the interactions of M^+, M^{2+}, and M^{3+} metal ions with polyalanine peptides. The abundances of the Ala_n+M^{m+} complexes are $M^+ > M^{2+} > M^{3+}$, with no complexes observed for M^{3+}. Ion mobility measurements and MD simulations for the Ala_n+M^+ complexes with $M^+ = Li^+$, Na^+, K^+, Cs^+, and Rb^+ indicate that the polyalanine peptide is helical with the metal ion coordinated to backbone CO groups at the C-terminus. The conformation of the complex is determined by a balance between maximizing the metal coordination and minimizing the disruption to the α-helical regions (increasing the length of the helix increases the interaction between the helix macrodipole and the charge on the metal ion). For the singly charged metal ions the balance is shifted toward minimizing the disruption of the helix.

For the Ala_n+M^{2+} complexes with $M^{2+} = Mg^{2+}$, Ca^{2+}, Sr^{2+}, and Ba^{2+} the ion mobility measurements and MD simulations show that the polyalanine peptide is helical in the Ala_n+M^{2+} complexes, but with substantial disruption at the C-terminus where the metal ion is bound. The lowest energy conformation found for Ala_n+Ca^{2+} has around eight residues at the C-terminus unraveled from a helical arrangement and wrapped around the metal ion to form a coordination shell. The constraints posed by the backbone prevent the peptide from forming an ideal coordination shell around the metal, and several of the backbone CO groups at the C-terminus do not point directly at the metal ion.

Acknowledgment. We gratefully acknowledge the support of the National Institutes of Health.

References and Notes

(1) Hofmeister, F. *Arch. Exp. Pathol. Pharmakol.* **1888**, *24*, 247−260.
(2) von Hippel, P. H.; Wong. K. Y. *J. Biol. Chem.* **1965**, *240*, 3909−3923.
(3) Friend, S. H.; Gurd, F. R. N. *Biochemistry* **1979**, *18*, 4612−4619.
(4) Goto, Y.; Fink, A. L. *Biochemistry* **1989**, *28*, 945−952.
(5) Stigter, D.; Dill, K. A. *Biochemistry* **1990**, *29*, 1262−1271.
(6) Ghadiri, M. R.; Choi, C. *J. Am. Chem. Soc.* **1990**, *112*, 1630−1632.
(7) Ruan, F.; Chen, Y.; Hopkins, P. B. *J. Am. Chem. Soc.* **1990**, *112*, 9403−9404.
(8) Ghadiri, M. R.; Soares, C.; Choi, C. *J. Am. Chem. Soc.* **1992**, *114*, 4000−4002
(9) Pessi, A.; Bianchi, E.; Crameri, A.; Venturini, S.; Tramontano, A.; Sollazzo, M. *Nature* **1993**, *362*, 367−369.
(10) Siedlecka, M.; Goch, G.; Ejchart, A.; Sticht, H.; Bierzynski, A. *Proc. Natl. Acad. Sci. U.S.A.* **1999**, *96*, 903−908.
(11) Cheng, R. P.; Fisher, S. L.; Imperiali, B. *J. Am. Chem. Soc.* **1996**, *118*, 11349−11356.
(12) DeGrado, W. F.; Summa, C. M.; Pavone, V.; Nastri, F.; Lombardi, A. *Annu. Rev. Biochem.* **1999**, *68*, 779−819.
(13) Kelso, M. J.; Hoang, H. N.; Appleton, T. G.; Fairlie, D. P. *J. Am. Chem. Soc.* **2000**, *122*, 10488−10489.
(14) Di Costanzo, L.; Wade, H.; Geremia, S.; Randaccio, L.; Pavone, V.; DeGrado, W. F.; Lombardi, A. *J. Am. Chem. Soc.* **2001**, *123*, 12749−12757.
(15) Klassen, J. S.; Anderson, S. G.; Blades, A. T.; Kebarle, P. *J. Phys. Chem.* **1996**, *100*, 14218−14227.
(16) Ryzhov, V.; Dunbar, R. C.; Cerda, B.; Wesdemiotis, C. *J. Am. Soc. Mass. Spectrom.* **2000**, *11*, 1037−1046.
(17) Jockusch, R. A.; Lemoff, A. S.; Williams, E. R. *J. Am. Chem. Soc.* **2001**, *123*, 12255−12265.
(18) Wyttenbach, T.; Witt, M.; Bowers, M. T. *J. Am. Chem. Soc.* **2000**, *122*, 3458−3464.
(19) Grese, R. P.; Gross, M. L. *J. Am. Chem. Soc.* **1990**, *112*, 5098−5104.
(20) Reiter, A.; Adams, J.; Zhao, H. *J. Am. Chem. Soc.* **1994**, *116*, 7827−7838.
(21) Hu, P.; Sorensen, C.; Gross, M. L. *J. Am. Soc. Mass Spectrom.* **1995**, *6*, 1079−1085.
(22) Li, H.; Siu, K. W. M.; Guevremont, R.; Le Blanc, J. C. Y. *J. Am. Soc. Mass Spectrom.* **1997**, *8*, 781−792.
(23) Nemirovskiy, O. V.; Gross, M. L. *J. Am. Soc. Mass Spectrom.* **1998**, *9*, 1020−1028.
(24) Wyttenbach, T.; Bushnell, J. E.; Bowers, M. T. *J. Am. Chem. Soc.* **1998**, *120*, 5098−5103.

(25) Nemirovskiy, O. V.; Gross, M. L. *J. Am. Soc. Mass Spectrom.* **2000**, *11*, 770−779.
(26) Nemirovskiy, O. V.; Ramanathan, R.; Gross, M. L. *J. Am. Soc. Mass Spectrom.* **1997**, *8*, 809−812.
(27) Nemirovskiy, O. V.; Giblin, D. E.; Gross, M. L. *J. Am. Soc. Mass Spectrom.* **1999**, *10*, 711−118.
(28) Hudgins, R. R.; Mao, Y.; Ratner, M. A.; Jarrold, M. F. *Biophys. J.* **1999**, *76*, 1591−1597.
(29) Kohtani, M.; Kinnear, B. S.; Jarrold, M. F. *J. Am. Chem. Soc.* **2000**, *122*, 12377−12378.
(30) Kinnear, B. S.; Hartings, M. R.; Jarrold, M. F. *J. Am. Chem. Soc.* **2001**, *123*, 5660−5667.
(31) Mason, E. A.; McDaniel, E. W. *Transport Properties of Ions in Gases*, Wiley: New York, 1988.
(32) Kolafa, J. http://www.icpf.cas.cz/jiri/macsimus/default.htm.
(33) Kohtani, M.; Jarrold, M. F. *J. Am. Chem. Soc.* **2002**, *124*, 11148−11158.
(34) Kinnear, B. S.; Kaleta, D. T.; Kohtani, M.; Hudgins, R. R.; Jarrold, M. F. *J. Am. Chem. Soc.* **2000**, *122*, 9243−9256.
(35) Hay, P. J.; Wadt, W. R. *J. Chem. Phys.* **1985**, *82*, 299−310.
(36) Strynadka, N. C. J.; James, M. N. G. *Annu. Rev. Biochem.* **1989**, *58*, 951−999.
(37) Cotton, F. A.; Wilkinson, G.; Murillo, C. A.; Bochmann, M. *Advanced Inorganic Chemistry*, 6th ed.; Wiley: New York, 1999.
(38) See, for example: Stace, A. J. *J. Phys. Chem. A* **2002**, *106*, 7993−8005.
(39) Shvartsburg, A. A. *J. Am. Chem. Soc.* **2002**, *124*, 7910−7911.